

Published in final edited form as:

Langmuir. 2005 December 20; 21(26): 12327–12332.

The Influence of PEG Architecture on Protein Adsorption and Conformation

Roger Michel^{1,2}, Stephanie Pasche³, Marcus Textor³, and David G. Castner^{*,1,2}

¹Department of Bioengineering, National ESCA and Surface Analysis Center for Biomedical Problems, Box 351750 University of Washington, Seattle, WA, USA ²Department of Chemical Engineering, National ESCA and Surface Analysis Center for Biomedical Problems, Box 351750 University of Washington, Seattle, WA, USA ³Laboratory for Surface Science and Technology, Swiss Federal Institute of Technology, Zurich, Switzerland

Abstract

Poly(L-lysine)-*g*-poly(ethylene glycol) (PLL-*g*-PEG) copolymers with various grafting ratios were adsorbed to niobium pentoxide-coated silicon wafers and characterized before and after protein adsorption using X-ray photoelectron spectroscopy (XPS) and time-of-flight secondary ion mass spectrometry (ToF-SIMS). Three proteins of different sizes, myoglobin (16 kD), albumin (67 kD), and fibrinogen (340 kD), were studied. XPS was used to quantify the amount of protein adsorbed to the bare and PEGylated surfaces, ToF-SIMS and principal component analysis (PCA) of SIMS intensities were used to study protein conformational changes. The smallest protein, myoglobin, generally adsorbed in higher numbers than the much larger fibrinogen. Protein adsorption was lowest on the surfaces with the highest PEG chain surface density, and increased as the PEG layer density decreased. The highest adsorption was found on lysine-coated and bare niobium surfaces. ToF-SIMS and PCA data evaluation provided further information on the degree of protein denaturation, which, for a particular protein, were found to decrease with increasing PEG surface density and increase with decreasing protein size.

Keywords

protein; adsorption; conformation; niobium oxide; poly(ethylene glycol); PEG; lysine; ToF-SIMS; XPS

Introduction

Protein adsorption to artificial implant surfaces is generally fast and nonspecific, leading to denatured protein that can cause a cascade of undesired events, known as the Foreign Body Reaction.^{1, 2} The investigation of these events, including knowledge of the conformational state of the proteins involved, is vital to improving performance of implants and eliminating problems such as infections and inflammatory responses.^{3, 4}

Poly(ethylene glycol) (PEG) has been a key polymer in reducing or eliminating protein adsorption to surfaces,^{5–9} however there are a multitude of other chemistries^{8, 10, 11} available

*Corresponding Author: David G. Castner, Director, National ESCA and Surface Analysis Center for Biomedical Problems, Departments of Chemical and Bioengineering, Box 351750, University of Washington, Seattle, WA 98195-1750. Email: castner@nb.engr.washington.edu Tel: 206-685-1229. Fax: 206-543-3778.

today. While completely nonfouling properties are desired in cases such as vascular stents and artificial heart valves,¹² integration of an implant in applications such as hip prosthesis shafts relies on surfaces that interact actively with cells and tissue.¹³ Therefore, PEG layers with functional end-groups have been used to elicit desired cellular responses.^{14, 15} Similarly, specific protein interaction are exploited in the proteomics biosensor area, where biospecific protein interaction can be achieved by covalently binding proteins or antibodies to PEG in a background of nonfouling PEG.^{16, 17} Such multi-step, rather complex immobilization protocols often suffer from insufficient reproducibility and high costs. It would be attractive to have at hand a simple one-step process allowing proteins to adsorb to the surface in defined concentration and with fully active and native conformation to trigger desired integration of the implant with the body.

This study focuses on the effect of specific alteration of PEG interface architecture on the adsorption and denaturation of proteins. Conformational changes of protein adsorbed to synthetic surfaces are of great relevance and have been studied on various surfaces.¹⁸⁻²² Poly (L-lysine)-*g*-poly(ethylene glycol) (PLL-*g*-PEG) is a cationic graft-copolymer that has been shown to adsorb to negatively charged surfaces such as many metal oxides and tissue culture polystyrene, thereby rendering them protein resistant.^{23, 24} Investigations of PLL-*g*-PEG layers by angle-resolved X-ray photoelectron spectroscopy (XPS) suggest that the poly-L-lysine is bound to the negatively charged surfaces with the PEG chains protruding away from the surface.²⁴ The grafting ratio (number of lysine monomers to PEG chains) can be easily and systematically varied by using appropriate ratios of the reacting reagents during the copolymer synthesis. A PLL-*g*-PEG graft copolymer with a graft ratio of 3.5, a PLL backbone of 20 kD, and PEG side chains of 2 kD, has been shown to render metal oxide surfaces (TiO₂, Nb₂O₅) resistant to protein adsorption from human blood serum,^{23, 24} as well as hinder cell attachment.²⁵⁻²⁷ However, with grafting ratios above 4-4.5, a steady increase of protein adsorbed mass has been reported and is correlated with decreasing PEG chain surface densities.²⁸⁻³⁰

Time-of-flight secondary ion mass spectrometry (ToF-SIMS) analyzes positively and negatively charged secondary ions and provides information about the surface elemental and chemical composition of the top 10-20 Å. As the analyzing depth is smaller than the dimensions of most proteins, static ToF-SIMS is sensitive to the conformation and orientation of adsorbed proteins.^{18, 22, 31, 32} Characteristic mass peaks generated by the fragmentation of amino acids have been assigned to specific amino acids and principal component analysis (PCA) was utilized to separate different proteins,^{33, 34} as well as differences in protein conformation.^{18, 22, 32}

This study examines protein adsorption to and conformational changes at niobia surfaces without and with adsorbed monolayers of PLL and PLL-*g*-PEG. PLL-*g*-PEG co-polymers with different grafting ratios (Lys/PEG) along with three proteins of different sizes: myoglobin (16 kD), albumin (67 kD), and fibrinogen (340 kD) were used. Niobia was used as the substrate surface because its high negative charge density at neutral pH provides excellent PLL-*g*-PEG adlayer stability and consistency.³⁵ The objectives of this study were to determine the relationship between PEG surface density, adsorbed protein mass and degree of protein conformational changes. The hypothesis was that surface PEGylation reduces not only the amount of proteins adsorbed, but also can reduce the degree of protein unfolding and denaturing. The degree of denaturing is expected to depend on both the type of protein and the surface density of the PEG chains.

Materials and Methods

PLL-g-PEG synthesis

PLL-g-PEG polymers were synthesized from a stoichiometric mixture of poly(L-lysine) hydrobromide (PLL) (Sigma, USA, molecular weight 15-30 kDa, polydispersity 1.1-1.3) and an N-hydroxysuccinimidyl ester of methoxy-terminated poly-(ethylene glycol) (mPEG-SPA) (Nektar, USA, 2 kDa, polydispersity < 1.05). Poly(L-lysine) was dissolved in a 50 mM sodium tetraborate (Sigma, USA) buffer solution (pH 8.5) in a concentration corresponding to 100 mM monomeric lysine. The solution was filter sterilized (0.22 μ m pore size filter, Millex-GV, Sigma-Aldrich, Switzerland). The mPEG-SPA was then added to the solution, and the mixture was stirred for 6 h at room temperature. Subsequently, the reaction mixture was dialyzed (Spectra-Por, molecular weight cutoff size 6-8 kDa, Spectrum Laboratories, Inc., USA) for 48 h against deionized water, changing the water after 24 h. The product was freeze dried and stored at -20°C before use. Further details regarding the synthesis protocol have been published previously.²⁴ The PLL-g-PEG product was characterized by ^1H NMR spectroscopy, using D_2O as a solvent on a 500-MHz Bruker instrument. A bulk value of the grafting ratio was determined from the NMR spectra.¹⁶ Choosing the correct stoichiometric ratio of Lys/PEG allowed for synthesis of PLL-g-PEG with graft ratios of 3.5, 10.1, and 22.6.

Other Chemicals

4-(2-hydroxyethyl)piperazine-1-ethanesulfonic acid (HEPES), bovine serum albumin, bovine plasma fibrinogen and horse heart myoglobin, as well as all organic solvents, were purchased from Sigma, USA, and used without further purification. 10x phosphate buffered saline (PBS) solution (EMD Biosciences, USA) was diluted with ultrapure water (18 M Ω , Modulab Analytical, US Filter Corporation, TX) to 1x concentration, and the pH was adjusted to 7.4 with 1N HCl or 1N NaOH when necessary.

Substrates and Surface Modification

Nb_2O_5 (12 nm) was sputter-coated onto silicon wafers (WaferNet GmbH, Germany) using reactive magnetron sputtering (PSI, Villigen, Switzerland), then diced into $1\times 1\text{ cm}^2$ squares.

The Nb_2O_5 samples were then sonicated in acetone, dichloromethane, methanol and ultrapure water for 10 min each, followed by 30 min of ozone cleaning (UVOCS Inc. Montgomeryville, PA). Cleaned samples were then transferred to a 24 well plate (Falcon Multiwell, VWR Scientific, PA) and immersed in 1 mg/mL solution of PLL or PLL-g-PEG in 10 mM HEPES buffer solution (adjusted to pH 7.4 with a 6 M NaOH). After 30 min of immersion, the modified samples were rinsed in the well plates twice with HEPES and twice with PBS buffer. The different surface modified Nb_2O_5 samples were then subjected to a 0.1 mg/ml protein solution for 2 h at room temperature.

After adsorption, the samples were rinsed following the solution displacement protocol described previously,³⁶ to avoid transferring protein from the air-water interface to the surface. The samples were then rinsed twice in PBS and three times in ultrapure water to remove loosely bound protein and buffer salts. They were dried in air and stored under nitrogen until analysis.

XPS Analysis

XPS spectra were acquired on Surface Science Instruments X-Probe and S-Probe instruments. Each of these systems is equipped with a monochromatized aluminum $\text{K}\alpha$ x-ray source, an electron flood gun for charge neutralization, and a hemispherical electron energy analyzer. All survey and detail scans for compositional analyses were acquired at a pass energy of 150 eV, and all high-resolution scans were acquired at a pass energy of 50 eV. Compositional analyses (0-1100 eV) and high resolution scans of the C 1s region were carried out on all samples. The

take-off-angle (the angle between the analyzer and the surface normal) was kept at 55 degrees for all samples analyzed. Data treatment was performed on the Service Physics ESCAVB data reduction software. (see 37 for details on XPS atomic percent calculation.) At least two replicates of each sample type were analyzed, with three spectra acquired on each replicate.

ToF-SIMS Analysis

A Model 7200 Physical Electronics instrument (PHI, Eden Prairie, MN) was used for static ToF-SIMS data acquisition. The instrument has an 8 keV Cs⁺ ion source, a reflectron time-of-flight mass analyzer, chevron type multichannel plates (MCP), and a time-to-digital converter (TDC). Positive secondary ions mass spectra were acquired over a mass range from $m/z = 0-500$. Negative ion ToF-SIMS spectra were not considered in this study due to their lower information content and lack of unique peaks for different amino acids.³⁸ The area of analysis for each spectrum was $100\ \mu\text{m} \times 100\ \mu\text{m}$, and the total ion dose used to acquire each spectrum was less than 2×10^{12} ions/cm². The mass resolution ($m/\Delta m$) of the secondary ion peaks in the positive spectra was typically between 4000 and 6000. The ion beam was moved to a different spot on the sample for each spectrum. The mass scales of the positive ion spectra were calibrated using to the CH₃⁺, C₂H₃⁺, C₃H₅⁺, and C₅H₁₀N⁺ peaks before further analysis. At least two replicates were analyzed for each sample type, with three spectra acquired on each replicate.

Principal Components Analysis (PCA)

Prior to multivariate analysis, two peak sets were generated from all of the samples: 1) a “complete” peak set taking into account all peaks with intensities above 100 cts in the 0-200 m/z region, and 2) a “reduced” peak set including only selected amino acid fragments. The selected peaks were then normalized to the total ion intensity to account for fluctuations in secondary ion yield between different spectra. PCA was then employed to analyze the positive ToF-SIMS spectra using PLS Toolbox v. 2.0 (Eigenvector Research, Manson, WA) for MATLAB (The MathWorks, Inc., Natick, MA). All spectra were mean-centered before running PCA. PCA was used to determine the linear combination of peaks that capture the highest degree of variation in a dataset.³⁹

Results and Discussion

The surfaces and proteins analyzed in this study are illustrated in Figure 1. Niobium pentoxide (Nb₂O₅) was used as a substrate and was modified by adsorption of poly(L-lysine) (PLL) and PLL-*g*-PEG at grafting ratios (Lys monomers per PEG side chain) of 3.5, 10.1, and 22.6 respectively. The adsorption of PLL-*g*-PEG onto niobia has been characterized previously.^{23, 28, 30} Single protein solutions of myoglobin (16 kD), albumin (67 kD), and fibrinogen (340 kD) at a concentration of 0.1 mg/ml were then exposed to the five different surfaces, using a previously described procedure.⁴⁰ A graph of the anticipated adsorption scenarios for one given sample type and the three proteins is shown in Figure 1.

XPS Analysis

Table 1 shows the XPS elemental composition of the bare and surface-modified Nb₂O₅ samples. Only niobium, carbon, oxygen and nitrogen were detected by XPS. The bare, cleaned niobium surface exhibits the highest levels of niobium and oxygen, although some carbon is present due to adventitious hydrocarbon contamination. Upon immersion of the Nb₂O₅ in the PLL and PLL-*g*-PEG solutions, the surfaces became coated with the polycationic polymers, displacing the hydrocarbon overlayer.²³ Nitrogen, indicative of the PLL, decreased steadily from 4.5% for a PLL overlayer, to 2.6% for the PLL-*g*[3.5]-PEG layer with the highest PEG surface density. Similarly, the amount of niobium detected decreased gradually from the uncoated Nb₂O₅ to the PLL and PLL-*g*-PEG coated overlayers. This is a consequence of attenuation of the substrate photoelectrons by the polymeric overlayer. The polymer thickness

increases with the degree of PEGylation, as schematically represented in Figure 1. The oxygen concentrations trend followed expectation with the lowest value measured for the PLL-coated Nb₂O₅ surface, and increasing for the PLL-g-PEG coated samples because of the high oxygen concentration in PEG.

The quantitative XPS data for the five different surfaces after exposure to solutions of myoglobin, albumin, and fibrinogen are also shown in Table 1. The average nitrogen concentrations are shown with standard deviations for nine measurements (three replicates with three spots per replicate). The error inherent in XPS nitrogen measurements of protein films is typically ± 0.5 at.%. Fibrinogen, the largest protein used in this study, exhibited 14% nitrogen when adsorbed onto the bare surface, indicative a full protein monolayer is formed.⁴¹ The smaller proteins, myoglobin and albumin, exhibited lower nitrogen concentrations when adsorbed to the bare niobium pentoxide surface (10.7% and 8.6%, respectively). This is believed to be due to the smaller size of the protein, which would yield a protein layer with a thickness that is smaller than the XPS sampling depth. With the exception of the bare surface, the nitrogen signals originate from both the interfacial PLL or PLL-g-PEG layer as well as the adsorbed proteins. Therefore, the nitrogen values of the modified surfaces measured before protein adsorption were subtracted from the overall nitrogen signal, to deduce the nitrogen contribution due to the adsorbed protein. Due to the attenuation of photoelectrons traveling through the adsorbed protein overlayer, the nitrogen signal of the underlying PLL and PLL-g-PEG is reduced on the protein covered samples. Therefore, to determine the true nitrogen contribution by the proteins, the nitrogen signal was corrected. This was done by evaluating the decrease in the Nb signal of niobia substrate for the PEG/PLL versus the PEG/PLL/protein samples. This correction increased the nitrogen concentration by <40% for the samples used in this study. The equation used for determining the “true” nitrogen signal from the protein overlayer was:

$$N_{Att} = N_{Prot} - N_{Sub} (Nb_{Prot}/Nb_{Sub}) \quad (1)$$

where N_{Att} is the corrected nitrogen value for each sample type, N_{Sub} is the nitrogen atomic % (at.%) of the substrate sample, N_{Prot} the nitrogen at.% in the protein samples, Nb_{Sub} the niobium at.% occurring from the substrate samples and Nb_{Prot} the at.% of the niobium in the protein samples.

Figure 2 shows the nitrogen concentrations after subtraction of the PLL contributions. At the highest grafting density g of 3.5, only trace amounts of nitrogen were observed (<1 at.%). This is in good agreement with earlier studies demonstrating the very high protein resistance of this type of polymer layer.²⁸ For the surfaces covered by the two polymers with the higher grafting ratios, i.e. with reduced PEG surface densities compared to the $g = 3.5$ polymer, the nitrogen concentrations increased with increasing g value and was highest on the PLL-coated and bare surfaces. The largest protein (fibrinogen) had the highest nitrogen signals among the three proteins on all samples. While similar amounts of albumin and fibrinogen adsorbed to the bare and PLL-coated surfaces, significantly more myoglobin adsorbed to the bare, negatively charged Nb₂O₅ compared to the positively charged PLL-coated surface. The reason may be that myoglobin has a higher point of isoelectric charge (PI = 7.0) than fibrinogen (PI = 5.5) or albumin (PI = 5.5) and is therefore less negatively charged (almost neutral) in the buffer solution (pH = 7.4).

When using the XPS nitrogen signal for the detection of adsorbed proteins, a larger sized protein will produce a higher nitrogen signal than a smaller sized protein. This is because the larger protein molecule has more nitrogen atoms in XPS sampling depth, thus the size of the protein needs to be taken into account. To convert the XPS signal to quantity that is more related to “number of molecules” basis, the following equation was used:

$$SC_{(n)} = SC_{(e)} * NF \quad (2)$$

where SC(n) = normalized surface coverage SC (e) = experimental surface coverage (in XPS at.% nitrogen)

$$NF = \frac{MW_{Fgn}}{MW_{proteinX}} \quad (\text{proteinX=Fgn, Alb, Myo}) \quad (2a)$$

The results from this normalization are shown in Figure 3. The equation does not account for the different shapes of the proteins or the exponential attenuation of the XPS signal with increasing protein thickness, but it does provide a reasonable estimate of the relative number of protein molecules. While this is only an approximation to the number of protein adsorbed, it demonstrates that on the modified and bare surfaces, more myoglobin (16 kD) molecules are adsorbed than fibrinogen (340 kD) molecules. In view of the architecture of the PEG/lysine, this supports the assumption that the underlying lysine can be more readily accessed by smaller than by larger proteins.

ToF-SIMS

Using the same matrix of bare, PLL- and PLL-g-PEG-coated Nb₂O₅ surfaces exposed to the three proteins, two peak sets were generated. The first set comprised all assigned peaks in the mass range from 0-200 m/z (cts >100), while the second set only used peaks unambiguously related to amino acid fragments from the protein overlayer.

Using the entire peak set, principal component 1 (PC1) captured 69% of the variance, as shown in Figure 4a. The PEG- and the Nb-containing fragments had positive PC1 loadings, while hydrocarbon and amino acids fragments had negative PC1 loadings (Figure 4b). The PC1 scores plot primarily separates the sample types by their surface modification. The lysine-coated and bare Nb₂O₅ surfaces adsorb the most protein, thus they have the highest negative scores since the amino acid fragments load negatively. The PEG surfaces, with the exception of the PLL-g[22.6]-PEG/fibrinogen sample, have positive PC1 scores consistent with the positive loadings of the PEG fragments. The scores plot clearly shows a dependency of the PEG-containing surfaces on PEG density (inversely proportional to the grafting ratio, ranging [3.5]>[10.1]>[22.6]). Interestingly, the niobium related peaks load positively, however at lesser intensity than the PEG or amino acid fragments. This trend is consistent with the XPS results that show lower niobium signals on the protein covered bare and lysine coated surfaces. Principal components two and higher captured only random variations in the sample types and did not provide any additional useful information.

To detect differences in the conformation of the adsorbed proteins, a peak set was chosen using only peaks resulting from amino acids. Starting with a previously generated amino acid peak set,⁴² additional peaks were removed that could also originate from the underlying PLL and PEG layers. A list of the peaks used in the amino acid peak set are shown in Table 2. Using this protein specific dataset, PCA was applied to all samples. PC1 captured 50.8% of the variance in the dataset, shown in Figure 5a. The loadings of PC1 (Figure 5b) show separation of most non-polar (labeled [n]) from polar (labeled [p]) amino acids. Conformational changes in proteins at surfaces using PCA and SIMS have been observed previously via the separation of polar and non-polar amino acids. This observation was made by using glutaraldehyde-protected, trehalose-protected and unprotected proteins.^{18, 22} As hydrophobic amino acids are more commonly found in the “interior” of the protein, a higher loading of these peaks may therefore indicate a higher degree of denaturation.³²

Figure 5a shows the PC1 scores plots. For each protein, the surface modification of Nb₂O₅ appears to influence the conformational state of the protein. As differences in surface concentration of the adsorbed protein has been taken into account by normalizing the peak set

to the sum of selected peaks, the differences in the detection of polar and non-polar peaks indicated a conformational change in the protein.

For each protein, the PLL-g[3.5]-PEG modification exhibits the most positive score. Our hypothesis for this observation is that the densest PEG layers prevent most of the protein from adsorbing to the surfaces. The proteins that still do adsorb retain a more native confirmation and this results in a relatively higher proportion of the polar amino acid fragments present at the protein surface. As the density of the PEG layers decreases, the values of the PC1 scores plot decrease. The lysine-coated and bare Nb₂O₅ substrates yield the most negative PC1 scores. This indicates the detection of more non-polar amino acids, associated with a more denatured protein state. This general decrease of the value of the scores plot with a decrease in PEG surface density is found across all three proteins. Myoglobin, the smallest protein in size (16 kD), exhibits more negative scores compared to the larger proteins albumin and fibrinogen. This could be attributed to the small size of this protein requiring less adhesive area for unfolding/denaturing compared to the larger proteins. A similar study that employed PEG conjugates linked to a polysulfonate film used fibronectin adsorption and fibroblasts attachment studies to provide indirect evidence that protein in a PEGylated environment had a higher biological activity.⁴³

Figure 5 shows the PCA scores and loadings for the combination of all three proteins on all surfaces. PCA experiments were also done on each individual protein on all surfaces. The resulting PCA scores and loadings from the individual protein data sets were similar to those in Figure 5 from the combined protein data set.

Since the samples were analyzed under ultra-high vacuum (UHV) water tends to leave the PEGylated and proteinaceous surfaces, which causes the proteins to denature. This denaturation can be prevented by rinsing the samples water with trehalose prior to drying and exposure to UHV.²² It is likely that the highly-grafted PEG copolymer in this study acts similar to trehalose and helps retain protein structure.

Conclusions

Nb₂O₅ coated silicon wafers were modified with PLL and PLL-g-PEG copolymers with various graft ratios and characterized before and after protein adsorption using XPS and ToF-SIMS. Three proteins of different sizes; myoglobin (16 kD), albumin (67 kD), and fibrinogen (340 kD), were studied. XPS was able to quantify protein adsorption to the modified surfaces and a correlation between PEG density and amount of protein and numbers of protein molecules was established. For any given PEG density, more myoglobin (absolute number of molecules) adsorbs to the surface. This difference may reflect the ability of the smaller proteins to adsorb in between the PEG chains. Fibrinogen, the largest protein analyzed, adsorbs in lowest numbers. ToF-SIMS and PCA were used for surface characterization as well as to study protein adsorption and conformational changes. PCA was able to separate the surface modifications and protein adsorption by using PEG, niobium, and amino acid fragments. A peak set containing peaks unambiguously attributed to amino acids from the protein overlayer was then used for further PCA analysis. A relationship between the types of surfaces and the loadings, separating most polar from non-polar amino acids, was detected. As the PEG-chain surface density decreases more non-polar amino acid were detected, indicating an increase in protein denaturation.

The next step for analyzing the conformational changes in proteins will be to combine the surface treatments with additional stabilizing agents (trehalose, glutaraldehyde) as well as using the PEG graft ratio to investigate size sequestering and exclusion of different sized proteins.

Acknowledgments

This research was supported by NIBIB grant EB-002027 to the National ESCA and Surface Analysis Center for Biomedical Problems (NESAC/BIO). The authors thank Dr. Matthew Wagner and Dr. Daniel Graham for expertise with PCA and Dr. Heather Canavan for insightful discussions.

References

1. Collier TO, Thomas CH, Anderson JM, Healy KE. *Journal of Biomedical Materials Research* 2000;49:141–145. [PubMed: 10559757]
2. Kao WJ, Hubbell JA, Anderson JM. *Journal of Materials Science-Materials in Medicine* 1999;10:601–605. [PubMed: 15347973]
3. Spector M, Cease C, Xia TL. *Critical Reviews in Biocompatibility* 1989;5:269–295.
4. Anderson JM, Miller KM. *Biomaterials* 1984;5:5–10. [PubMed: 6375747]
5. Bergstrom K, Holmberg K, Safranj A, Hoffman AS, Edgell MJ, Kozlowski A, Hovanes BA, Harris JM. *Journal of Biomedical Materials Research* 1992;26:779–790. [PubMed: 1527100]
6. Harris, MJ. *Poly(ethylene glycol) chemistry biotechnical and biomedical applications*. New York Plenum Press; New York: 1992.
7. Prime KL, Whitesides GM. *Journal of the American Chemical Society* 1993;115:10714–10721.
8. Kingshott P, Griesser HJ. *Current Opinion in Solid State & Materials Science* 1999;4:403–412.
9. Kingshott P, McArthur S, Thissen H, Castner DG, Griesser HJ. *Biomaterials* 2002;23:4775–4785. [PubMed: 12361616]
10. Ostuni E, Chapman RG, Holmlin RE, Takayama S, Whitesides GM. *Langmuir* 2001;17:5605–5620.
11. Glasmaster K, Larsson C, Hook F, Kasemo B. *Journal of Colloid and Interface Science* 2002;246:40–47. [PubMed: 16290382]
12. Park K, Shim HS, Dewanjee MK, Eigler NL. *Journal of Biomaterials Science-Polymer Edition* 2000;11:1121–1134. [PubMed: 11263803]
13. Migaud H, Jardin C, Fontaine C, Pierchon F, dHerbomez O, Duquennoy A. *Revue De Chirurgie Orthopedique Et Reparatrice De L Appareil Moteur* 1997;83:360–367. [PubMed: 9452810]
14. Bearinger JP, Castner DG, Healy KE. *Journal of Biomaterials Science-Polymer Edition* 1998;9:629–652. [PubMed: 9686332]
15. Tosatti S, Schwartz Z, Campbell C, Cochran DL, VandeVondele S, Hubbell JA, Denzer A, Simpson J, Wieland M, Lohmann CH, Textor M, Boyan BD. *Journal of Biomedical Materials Research Part A* 2004;68A:458–472. [PubMed: 14762925]
16. Huang NP, Voros J, De Paul SM, Textor M, Spencer ND. *Langmuir* 2002;18:220–230.
17. Nelson KE, Gamble L, Jung LS, Boeckl MS, Naeemi E, Golledge SL, Sasaki T, Castner DG, Campbell CT, Stayton PS. *Langmuir* 2001;17:2807–2816.
18. Xia N, May CJ, McArthur SL, Castner DG. *Langmuir* 2002;18:4090–4097.
19. Lhoest JB, Detrait E, van den Bosch de Aguilar P, Bertrand P. *Journal of Biomedical Materials Research* 1998;41:95–103. [PubMed: 9641629]
20. Keselowsky BG, Collard DM, Garcia AJ. *Journal of Biomedical Materials Research Part A* 2003;66A:247–259. [PubMed: 12888994]
21. Grainger DW, Pavon-Djavid G, Migonney V, Josefowicz M. *Journal of Biomaterials Science-Polymer Edition* 2003;14:973–988. [PubMed: 14661874]
22. Xia N, Castner DG. *Journal of Biomedical Materials Research Part A* 2003;67A:179–190. [PubMed: 14517875]
23. Kenausis GL, Voros J, Elbert DL, Huang NP, Hofer R, Ruiz-Taylor L, Textor M, Hubbell JA, Spencer ND. *Journal of Physical Chemistry B* 2000;104:3298–3309.
24. Huang NP, Michel R, Voros J, Textor M, Hofer R, Rossi A, Elbert DL, Hubbell JA, Spencer ND. *Langmuir* 2001;17:489–498.
25. Elbert DL, Hubbell JA. *Chemistry & Biology* 1998;5:177–183. [PubMed: 9545428]
26. Michel R, Lussi JW, Csucs G, Reviakine I, Danuser G, Ketterer B, Hubbell JA, Textor M, Spencer ND. *Langmuir* 2002;18:3281–3287.

27. Csucs G, Michel R, Lussi JW, Textor M, Danuser G. *Biomaterials* 2003;24:1713–1720. [PubMed: 12593952]
28. Pasche S, De Paul SM, Voros J, Spencer ND, Textor M. *Langmuir* 2003;19:9216–9225.
29. Pasche S, Textor M, Meagher L, Spencer ND, Griesser HJ. *Langmuir* 2005;21:6508–6520. [PubMed: 15982060]
30. Wagner MS, Pasche S, Castner DG, Textor M. *Analytical Chemistry* 2004;76:1483–1492. [PubMed: 14987107]
31. Wang H, Castner DG, Ratner BD, Jiang SY. *Langmuir* 2004;20:1877–1887. [PubMed: 15801458]
32. Tidwell CD, Castner DG, Golledge SL, Ratner BD, Meyer K, Hagenhoff B, Benninghoven A. *Surface and Interface Analysis* 2001;31:724–733.
33. Wagner MS, Castner DG. *Applied Surface Science* 2003;203:698–703.
34. Wagner MS, Horbett TA, Castner DG. *Biomaterials* 2003;24:1897–1908. [PubMed: 12615480]
35. Pasche S, Voros J, Griesser HJ, Spencer ND, Textor M. *J. Phys. Chem. B*. 2005Submitted
36. Horbett, TA. *Techniques of Biocompatibility Testing*. Williams, DF., editor. 2. CRC Press, Inc.; Boca Raton: 1986. p. 183-215.
37. Tyler BJ, Castner DG, Ratner BD. *Surface and Interface Analysis* 1989;14:443–450.
38. Mantus DS, Ratner BD, Carlson BA, Moulder JF. *Analytical Chemistry* 1993;65:1431–1438. [PubMed: 8517550]
39. Jackson, JE. *A User's Guide to Principal Components*. Wiley; New York: 1991.
40. Wagner MS, Castner DG. *Langmuir* 2001;17:4649–4660.
41. Paynter RW, Ratner BD, Horbett TA, Thomas HR. *Journal of Colloid and Interface Science* 1984;101:233–245.
42. Lhoest JB, Wagner MS, Tidwell CD, Castner DG. *Journal of Biomedical Materials Research* 2001;57:432–440. [PubMed: 11523038]
43. Thom VH, Altankov G, Groth T, Jankova K, Jonsson G, Ulbricht M. *Langmuir* 2000;16:2756–2765.

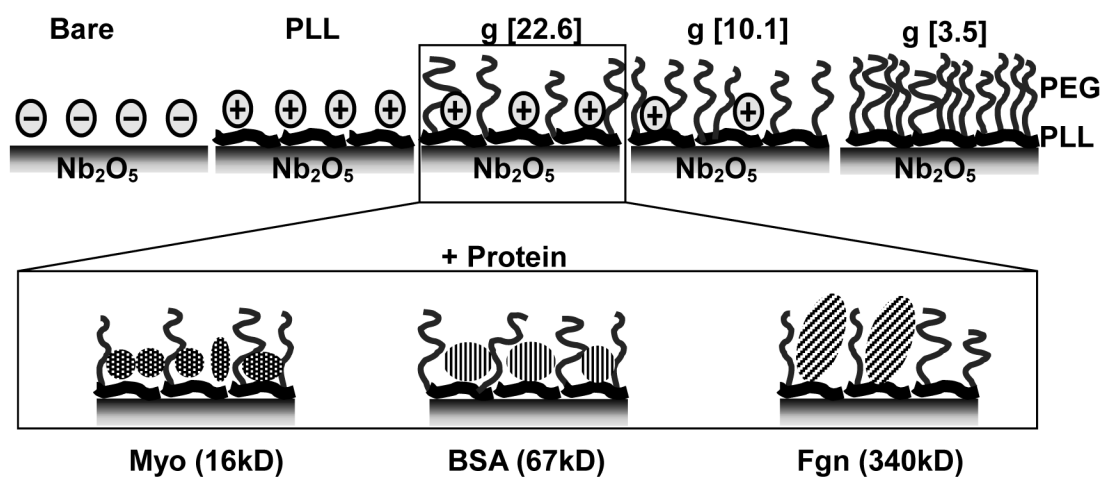


Figure 1. Surface modification and adsorption. Substrate Layer: Nb_2O_5 shown bare (top left), and modified with PLL, and PLL-g[22.6]-PEG, PLL-g[10.1]-PEG, and PLL-g[3.5]-PEG (top right). Protein Layer: Inset (bottom) shows proposed effect of protein size on adsorption to PLL-g[22.6]-PEG modified Nb_2O_5 surfaces.

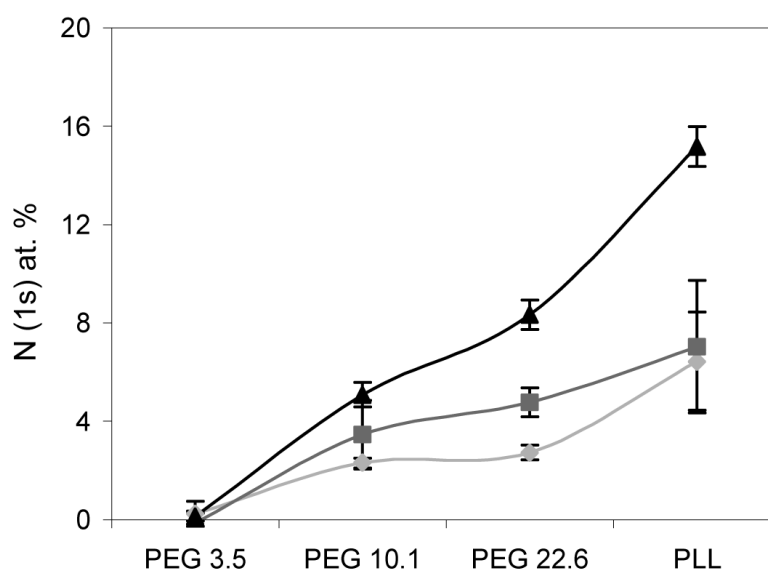


Figure 2.

Relative amount of adsorbed protein to surfaces as determined by XPS atomic % N1s after removing the PLL nitrogen contribution (see Eqn. 1). The amount of myoglobin (light grey), albumin (dark grey) and fibrinogen (black) are generally observed to increase with decreasing PEG density ($g[3.5] > [10.1] > [22.6]$). For any given surface modification, the highest atomic % N1s is observed for the largest size protein (fibrinogen), while the lowest amounts are observed from the smallest protein (myoglobin).

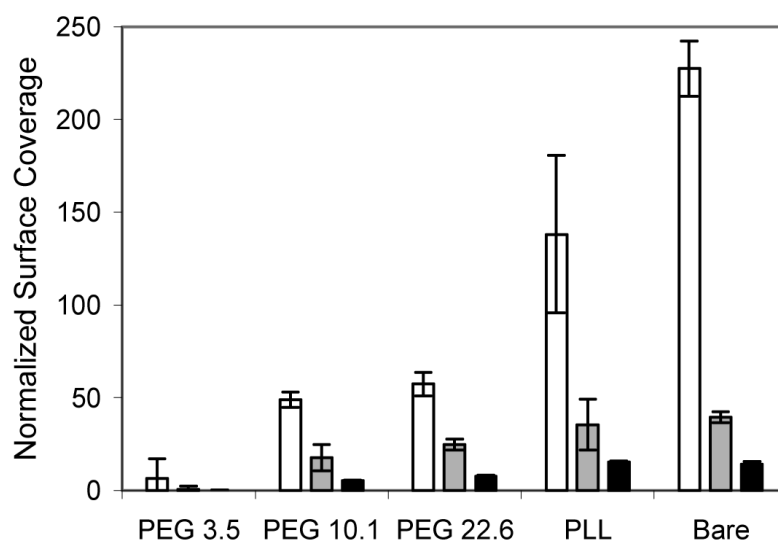


Figure 3.

XPS compositional data normalized to the size of the proteins (see Eqn 2). Once the N1s signal has been normalized to take into account the size of the proteins, it is observed that number of adsorbed protein molecules on a give substrate correlates with the molecular weight of the proteins: highest for the smallest protein (myoglobin, white), intermediate for albumin (grey), lowest for fibrinogen (black). The general trend of increasing number of protein molecules adsorbed with decreasing PEG density is observed.

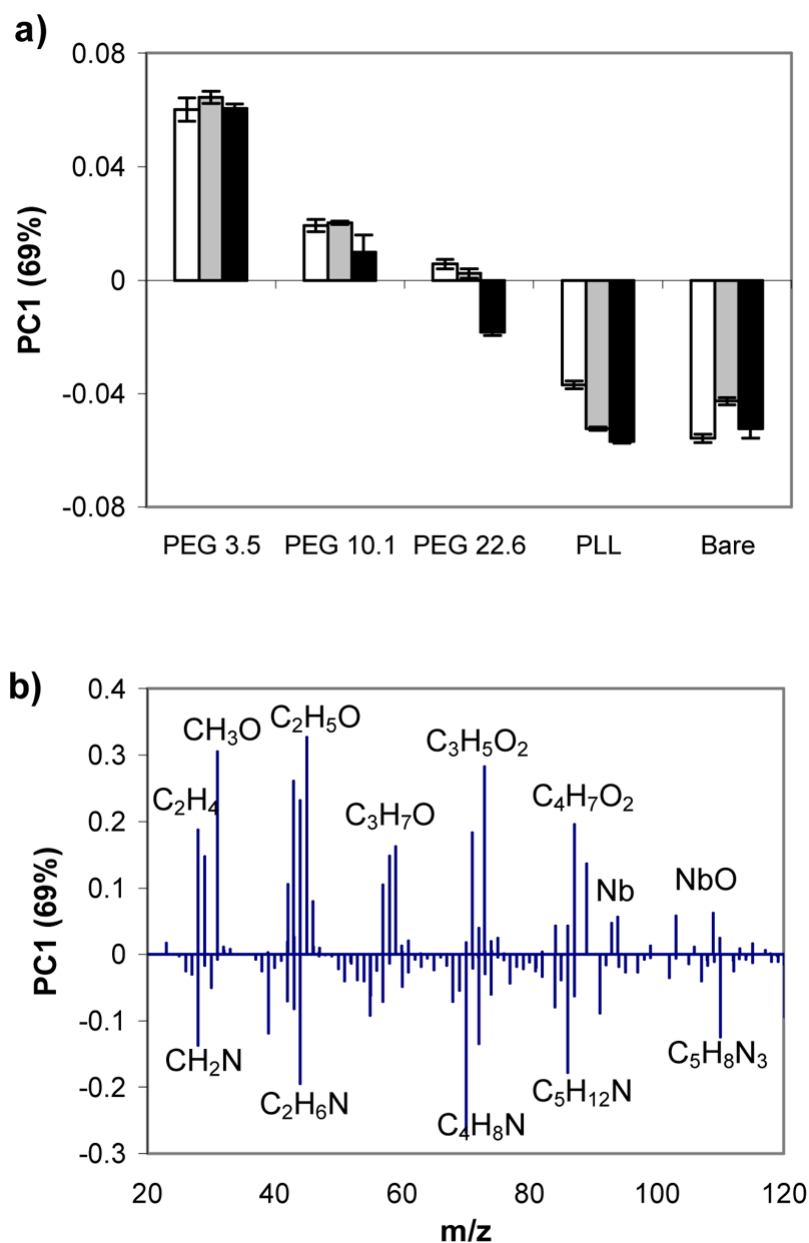
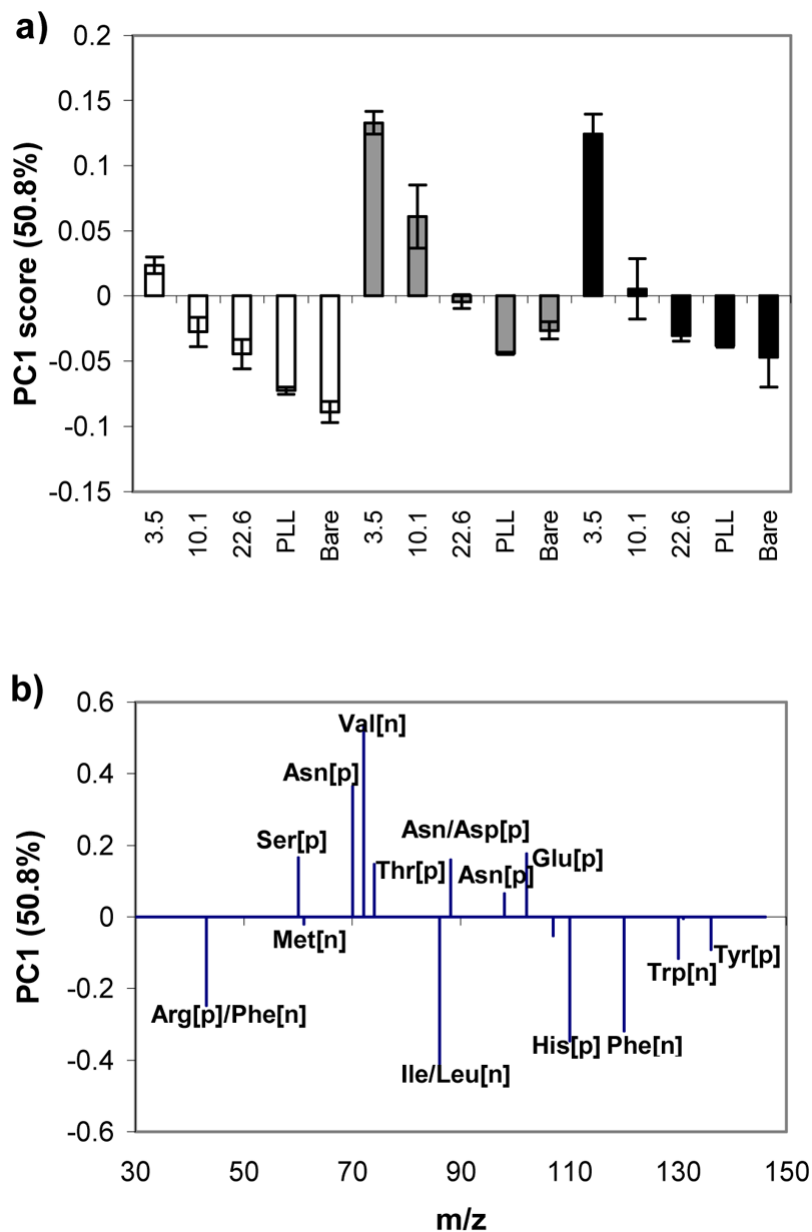


Figure 4.

PCA analysis of positive ion ToF-SIMS spectra obtained for myoglobin (white), albumin (grey) and fibrinogen (black) adsorbed to Nb_2O_5 , PLL and PLL-*g*-PEG treated surfaces. PC1 scores (a) and loadings (b) plots generated from a comprehensive peak set. PC1 separates the high-density [*g*=3.5] PEG-treated samples from the bare and PLL-coated samples. PEG and niobium related peaks are found to load positively (indicative of the higher PEG density). Fragments resulting from hydrocarbons as well as fragments from amino acid from the proteins load negatively, indicative of protein adsorption to the surfaces.

**Figure 5.**

PCA analysis of positive ToF-SIMS spectra obtained for myoglobin (white), albumin (grey) and fibrinogen (black) adsorbed to Nb₂O₅, PLL and PLL-g-PEG treated surfaces. PC1 scores (a) and loadings (b) plots generated from the selected amino acid peak set separate the high-density PEG samples from the bare and PLL-coated samples. The positive loaded fragments, (corresponding to samples with higher PEG densities) are mostly polar amino acids [p], while the negative loaded fragments are mainly non-polar amino acids [n] indicative of a more denatured protein conformation.

Table 1

XPS elemental composition of the bare, PLL, and PLL-g-PEG treated Nb₂O₅ surfaces (first group). Elemental composition of these surfaces after adsorption of myoglobin, albumin and fibrinogen are shown in groups 2-4.

	C 1s	O 1s	N 1s	Nb 2p
Nb ₂ O ₅ , PLL-g-PEG 3.5	44.2 ± 0.4	43.8 ± 0.2	2.6 ± 0.1	9.4 ± 0.3
Nb ₂ O ₅ , PLL-g-PEG 10.1	37.2 ± 0.4	46.5 ± 0.5	3.5 ± 0.0	12.8 ± 0.2
Nb ₂ O ₅ , PLL-g-PEG 22.6	35.6 ± 1.2	47.1 ± 0.8	4.0 ± 0.6	13.3 ± 0.1
Nb ₂ O ₅ , PLL	36.4 ± 1.4	45.1 ± 1.8	4.5 ± 0.7	14.0 ± 0.4
Nb ₂ O ₅ , Bare	23.0 ± 1.7	58.4 ± 1.2	0.0 ± 0.0	18.6 ± 0.5
Nb ₂ O ₅ , PLL-g-PEG 3.5, Myoglobin	42.6 ± 3.3	44.5 ± 2.1	3.0 ± 0.5	10.0 ± 1.2
Nb ₂ O ₅ , PLL-g-PEG 10.1, Myoglobin	39.7 ± 1.1	43.6 ± 1.0	5.4 ± 0.2	11.3 ± 0.3
Nb ₂ O ₅ , PLL-g-PEG 22.6, Myoglobin	40.0 ± 2.9	42.6 ± 2.4	6.1 ± 0.3	11.2 ± 0.4
Nb ₂ O ₅ , PLL, Myoglobin	42.1 ± 2.6	39.7 ± 2.1	9.3 ± 2.0	8.9 ± 1.5
Nb ₂ O ₅ , Bare, Myoglobin	49.7 ± 0.7	32.6 ± 0.9	10.7 ± 0.7	7.0 ± 0.4
Nb ₂ O ₅ , PLL-g-PEG 3.5, Albumin	41.8 ± 1.6	45.2 ± 1.3	2.7 ± 0.4	10.3 ± 0.6
Nb ₂ O ₅ , PLL-g-PEG 10.1, Albumin	41.7 ± 4.2	41.6 ± 4.2	6.3 ± 1.4	10.4 ± 1.4
Nb ₂ O ₅ , PLL-g-PEG 22.6, Albumin	44.8 ± 5.0	38.2 ± 4.6	7.6 ± 1.6	9.4 ± 1.9
Nb ₂ O ₅ , PLL, Albumin	50.2 ± 3.5	31.9 ± 3.2	9.7 ± 2.7	8.3 ± 3.0
Nb ₂ O ₅ , Bare, Albumin	45.8 ± 8.4	36.8 ± 6.1	7.8 ± 0.6	9.6 ± 2.1
Nb ₂ O ₅ , PLL-g-PEG 3.5, Fibrinogen	45.1 ± 1.2	43.4 ± 0.9	2.6 ± 0.2	8.9 ± 0.5
Nb ₂ O ₅ , PLL-g-PEG 10.1, Fibrinogen	42.7 ± 1.6	39.9 ± 0.6	7.7 ± 0.5	9.6 ± 0.7
Nb ₂ O ₅ , PLL-g-PEG 22.6, Fibrinogen	48.6 ± 0.9	33.7 ± 0.6	10.5 ± 0.6	7.2 ± 0.7
Nb ₂ O ₅ , PLL, Fibrinogen	61.5 ± 0.8	22.1 ± 0.8	15.5 ± 0.8	1.0 ± 0.6
Nb ₂ O ₅ , Bare, Fibrinogen	61.3 ± 2.2	23.0 ± 0.5	14.0 ± 1.3	1.4 ± 0.5

Table 2

Amino acid fragments used in the ToF-SIMS studies to examine protein conformation.

Summary of Characteristic Fragments Assigned to Amino Acids^(a)

Arginine (Arg, R)	43.0296	CH ₃ N ₂
Asparagine (Asn, N)	70.0293	C ₃ H ₄ NO
Asparagine (Asn, N)	88.0398	C ₃ H ₆ NO ₂
Asparagine (Asn, N)	98.0242	C ₄ H ₄ NO ₂
Aspartic Acid (Asp, D)	88.0398	C ₃ H ₆ NO ₂
Glutamine (Gln, Q)	84.0449	C ₄ H ₆ NO
Glutamic Acid (Glu, E)	84.0449	C ₄ H ₆ NO
Histidine (His, H)	110.0718	C ₅ H ₈ N ₃
Isoleucine (Ile, I)	86.0970	C ₅ H ₁₂ N
Leucine (Ile, L)	86.0970	C ₅ H ₁₂ N
Methionine (Met, M)	61.0112	C ₂ H ₅ S
Phenylalanine (Phe, F)	43.0296	CH ₃ N ₂
Phenylalanine (Phe, F)	120.0813	C ₈ H ₁₀ N
Serine (Ser, S)	60.0449	C ₂ H ₆ NO
Threonine (Thr, T)	74.0606	C ₃ H ₈ NO
Tryptophan (Trp, W)	130.0657	C ₉ H ₈ N
Tyrosine (Tyr, Y)	136.0762	C ₈ H ₁₀ NO
Valine (Val, V)	72.0813	C ₄ H ₁₀ N

^aFragments occurring from both the amino acids and the modified substrates (Nb₂O₅, PLL, PEG) were discarded.